Received 21 June; accepted 4 September 1985.

1. Shechtman, D., Blech, I., Gratias, D. & Cahn, J. W. *Phys. Rev. Lett.* **53**, 1951 (1984).
2. Shechtman, D. & Blech, I. *Metal Trans.* (in the press).
3. Levine, D. & Steinhardt, P. J. *Phys. Rev. Lett.* **53**, 2477 (1984).
4. Bak, P. *Phys. Rev. Lett.* **54**, 1517 (1985).
5. Levine, D. *et al. Phys. Rev. Lett.* **54**, 1520 (1985).
6. Mermin, N. D. & Trorian, S. M. *Phys. Rev. Lett.* **54**, 1524 (1985).
7. Heiney, P. A. *Nature* **315**, 178 (1985).
8. Pauling, L. *The Nature of the Chemical Bond* 3rd edn (Cornell University Press, Ithaca, 1960).
9. Adam, J. & Rich, J. B. *Acta crystallogr.* **7**, 813 (1954).
10. Pauling, L. & Marsh, R. E. *Proc. natn. Acad. Sci. U.S.A.* **36**, 112 (1952).
11. Claussen, W. F. *J. Chem. Phys.* **19**, 259, 662, 1425 (1951).
12. Samson, S. in *Structural Chemistry* and *Molecular Biology* (eds Rich, A. & Davidson, N.) 687-717 (Freeman, San Francisco, 1968).
13. Samson, S. *Nature* **195**, 259-262 (1962).
14. Samson, S. *Acta crystallogr.* **17**, 491 (1964).
15. Samson, S. *Acta crystallogr.* **19**, 401 (1965).
16. Pauling, L. *J. Am. chem. Soc.* **45**, 2777 (1923).
17. Bergman, G., Waugh, J. L. T. & Pauling, L. *Nature* **169**, 1057-1058 (1952); *Acta crystallogr.* **10**, 254 (1957).

Momentum flux in breaking waves

W. K. Melville & Ronald J. Rapp

Massachusetts Institute of Technology, Cambridge, Massachusetts 02139, USA

Wave breaking is believed to be important in air–sea interaction. Laboratory measurements[1] suggest that the momentum flux from the atmosphere to the ocean may be significantly enhanced by breaking and recent field measurements[2–4] have demonstrated the important role of breaking in bubble generation and gas transfer. It has long been speculated that the loss of momentum flux from the wave field due to breaking could act as a source of momentum for current generation[5] and Mitsuyasu[6] has drawn attention to the large discrepancy between the momentum flux from the wind and that carried by the waves, suggesting that the loss may be due to wave breaking. Here we present what we believe are the first well-controlled laboratory measurements of the momentum flux lost by wave breaking. These measurements are consistent with Mitsuyasu's hypothesis and recent measurements of wave growth, and support the conclusion that wave breaking plays an important role in momentum transfer across the air–sea interface.

Wave breaking may result from intrinsic instabilities of uniform surface waves[7,8], wave–current interaction[9], and the superposition and nonlinear interaction of spectral components of a random wave field. The breaking and white-capping associated with the modulation of the waves near the peak of the spectrum[3,10], (that is, with the tendency of the waves to occur in groups) is likely to be due to the latter mechanism. We simulated this condition in a wave channel[5,11] in which single isolated packets of waves were generated by superposition of Fourier components of equal amplitude a_0 at the wavemaker in a radian frequency band $(f_0 \pm \Delta f/2)$. The initial phase for each component was chosen to give constructive interference of linear surface waves at a point x_0 down the channel. This gives a nominal dimensionless duration of the packet at breaking of $2f_0/\Delta f$ wave periods. Dimensional reasoning then implies that the dimensionless wave amplitude a/a_0 and other variables will be functions of (xk_0, tf_0) with parametric dependence on $(a_0k_0, \Delta f/f_0, x_0k_0)$ where x is the distance down the channel, t is time and $k_0 = f_0^2/g$, the linear dispersion relationship for deep-water waves.

The parameters a_0k_0, $\Delta f/f_0$, x_0k_0, which are dimensionless measures of amplitude, bandwidth and phase, were varied in the ranges 0.1–0.5, 0.4–1.4 and 27.4–66.0, respectively. The water depth was 60 cm and f_0 was in the range 5.5–8.1 rad s^{-1}.

Figure 1 shows an example of the evolution of a wave packet at various stations down the channel. The incidence of breaking depends on the parameters above, most notably a_0. Figure 2 shows examples of single spilling and plunging events at specific values of a_0k_0. At other values of a_0k_0, multiple breaking waves were observed, and this led to consideration of losses due to

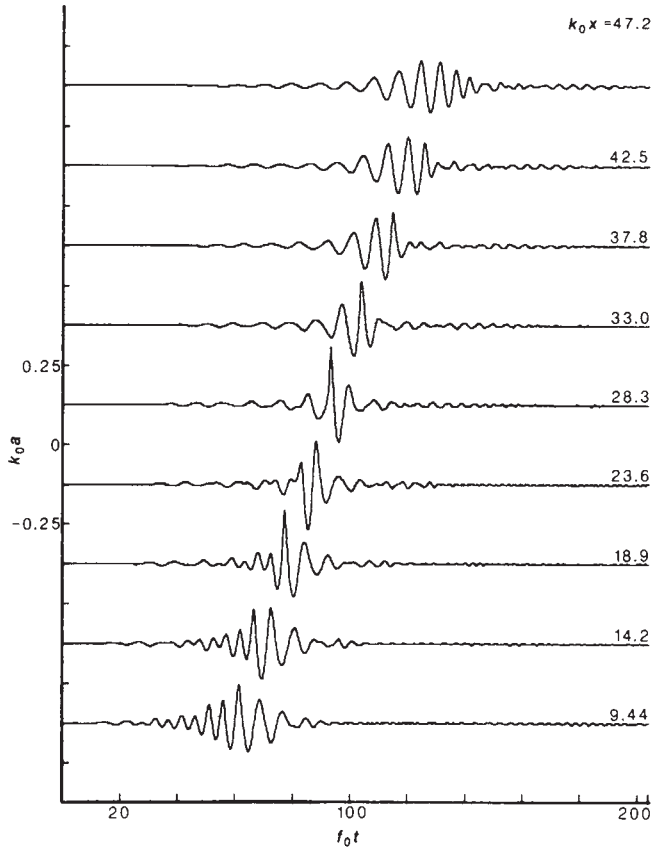

Fig. 1 Time series of surface displacement at stations down the wave channel for a spilling breaker: $f_0 = 6.79\ s^{-1}$, $\Delta f/f_0 = 0.73$, $x_0k_0 = 27.4$, $a_0k_0 = 0.30$. The time is normalized by f_0 and the amplitude by k_0. Breaking occurs at $xk_0 = 28$, where xk_0 is the normalized distance from the paddle.

'breaking' of the packet rather than single breaking waves. Indeed, multiple breaking events are observed in the field[3]. In these experiments the breaking process (whether single or multiple) was taken to be a 'black box' and the loss of excess momentum flux was evaluated by measuring the flux upstream and downstream of the breaking region.

For weakly nonlinear, slowly varying two-dimensional deep-water waves the excess momentum flux is proportional to a^2 (ref. 12). Thus we integrated a^2 during passage of the packet at various stations down the channel. Examples of this measure of integrated momentum flux, S, with distance down the channel are shown in Fig. 3 for incipient breaking, spilling and plunging events. The loss of momentum flux, ΔS, due to breaking is determined by taking the difference between the incipient breaking and breaking measurements downstream. The breaking region is clearly shown in this figure by a rapid decrease in S/S_0, the dimensionless excess momentum flux. The decline in S/S_0 prior to breaking is, we believe, due to the increasing influence of nonlinearity and strong modulation of the wave variables as the breakpoint is approached. Our use of the downstream differences, where S/S_0 is essentially constant, avoids its explicit consideration. We believe the oscillations in the breaking region are caused by rapid modulations of the wave variables which, as a consequence of dispersion, do not occur far upstream and downstream of this region. They are not accounted for in our approximation of the momentum flux, and are not relevant for our present purposes.

Results like those of Fig. 3 were collected for a range of parameters and used to determine the excess momentum flux loss due to breaking, $\Delta S/S_0$, as a function of a_0k_0, $\Delta f/f_0$, x_0k_0. An example is shown in Fig. 4 for fixed x_0k_0 for different amplitudes and bandwidths. This figure is typical of the data

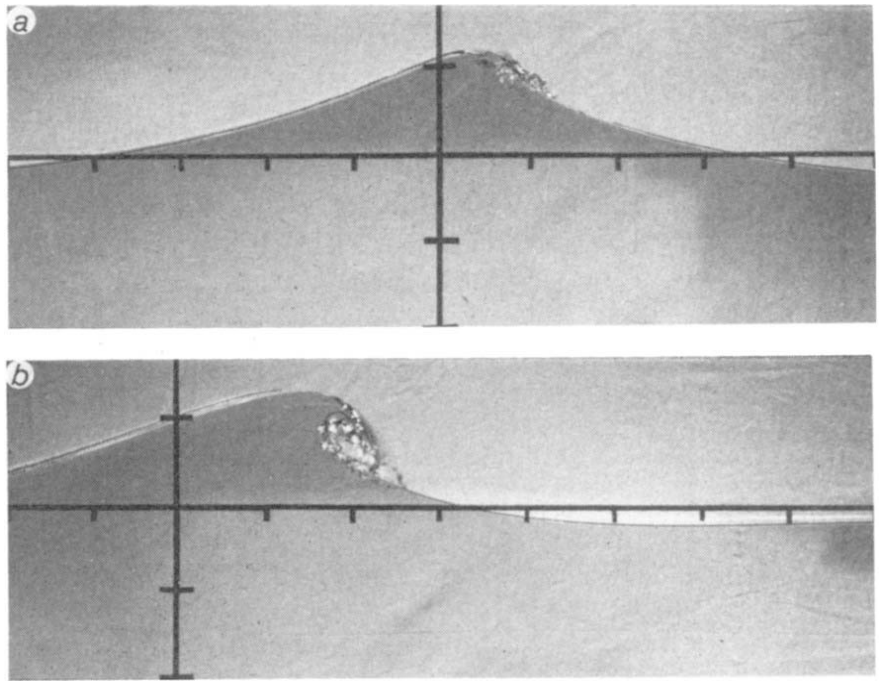

Fig. 2 Examples of single breaking waves for $f_0 = 5.53\ s^{-1}$, $\Delta f/f_0 = 0.73$, $x_0 k_0 = 27.4$. *a*, Spilling, $a_0 k_0 = 0.28$. *b*, Plunging, $a_0 k_0 = 0.35$. The marks are spaced at 10-cm intervals, and the upper boundary of the horizontal bar is at the still-water level.

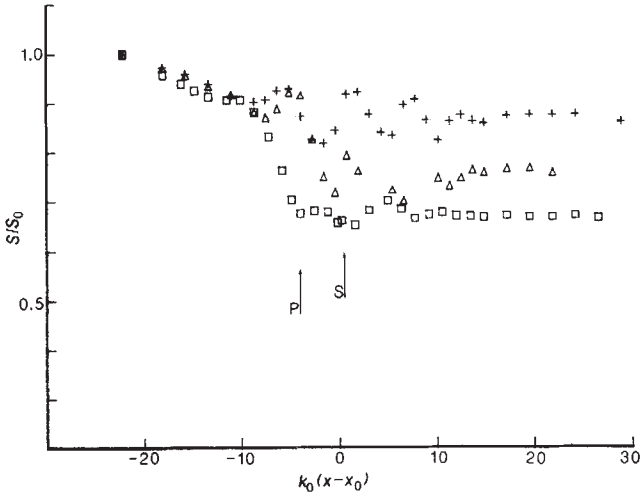

Fig. 3 Variance of the free surface displacement normalized by its upstream reference value at stations down the channel: $f_0 = 6.79\ s^{-1}$, $\Delta f/f_0 = 0.73$, $x_0 k_0 = 27.4$. The amplitude parameter $a_0 k_0$ is: 0.26, incipient breaking, +; 0.30, single spill, △; 0.39, single plunger, □. The normalized variance is approximately proportional to the excess momentum carried by the wave field past the measuring station, upstream and downstream of the breaking region. The actual breaking locations are marked by S (spilling) and P (plunging). The run denoted by △ is that shown in Fig. 1. The scatter in repeated measurements was within the size of the symbols.

Table 1 Estimates of $\Delta S/S$, the fractional increase of wave momentum flux due to wind forcing between breaking events

U_{10} (m s^{-1})	u_* (m s^{-1})	T (s)	c (m s^{-1})	u_*/c	$\bar{x}/\lambda$	$\Delta S/S$
6	0.21	2.6	4.1	0.05	20	0.04
12	0.48	3.1	4.8	0.10	13	0.09

Values determined according to equation (3) and data of refs 3 and 14. Variables are defined in the text.

collected and shows that the losses increase rapidly with increasing amplitude: 10% or more of the momentum flux carried by the packet may be lost through one breaking wave, and up to 20–30% from one multiple breaking event. The experiments show that the fractional loss of excess momentum from one wave packet due to one breaking event is in the range

$$\frac{\Delta S}{S_0} = 0(10^{-2} - 10^{-1}) \tag{1}$$

From wave growth measurements in deep water, Mitsuyasu[6] found that the divergence of the wave momentum flux inferred from direct measurements of wave growth in the laboratory is given by

$$\frac{dS}{dx} = 0.68\left[\frac{u_*^2}{c}\right]\frac{S}{\lambda} \tag{2}$$

where u_* is the friction velocity of the wind, c the phase speed of the waves, λ is wavelength and $0.1 \leq u_*/c \leq 1.0$. The coefficient 0.68 is within the range (0.5 ± 0.25) inferred by Plant's[13] extensive review of laboratory and field data. Mitsuyasu went on to show that dS/dx derived from the fetch relation for wind waves is an order of magnitude less than that given by equation (2), and suggested that a large fraction of this equation must then be balanced by wave breaking.

Now if $\Delta S/S \ll 1$, we may approximate equation (2) by its difference form

$$\frac{\Delta S}{S} = 0.68\left[\frac{u_*^2}{c}\right]\frac{\Delta x}{\lambda} \tag{3}$$

If $\Delta S/S$ over the distance between breaking events is comparable in magnitude to the fractional loss due to a breaking event, then we may state that the momentum lost due to breaking is comparable to that gained from the wind. As far as we are aware, the only measurements of the distance between breaking events (in the direction of the wind) are those of Thorpe and Humphries[3] who plotted $\lambda/\bar{x}$, the ratio of wavelength to mean distance between breaking waves, or the number of breaking waves per wave, versus the windspeed U_{10}, for $5 < U_{10} < 15\ m\ s^{-1}$. In this speed range, they found that $0.02 < \lambda/\bar{x} < 0.19$. Unfortunately, they only gave the phase speed c at two values of U_{10} and no explicit information on u_*. We may proceed to

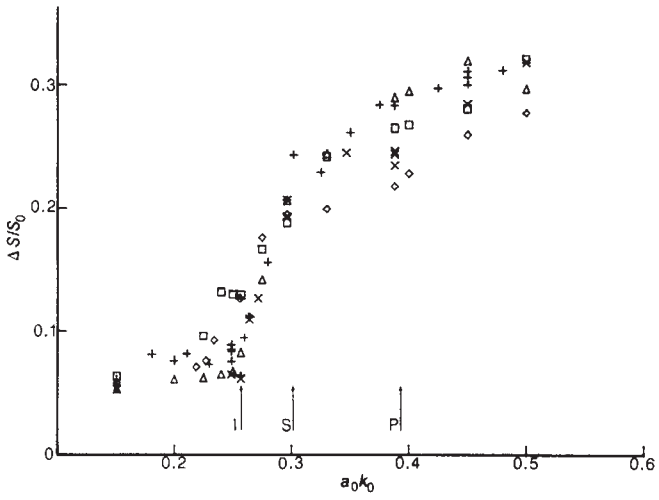

Fig. 4 Excess momentum lost from the wave field due to breaking as a function of the amplitude parameter, a_0k_0, for $\Delta f/f_0 = 0.4(\square)$, $0.6(\triangle)$, $0.73(+)$, $1.0(\times)$, $1.4(\diamond)$; $f_0 = 6.79\ s^{-1}$, $x_0k_0 = 27.4$. The arrows show the amplitudes for incipient breaking (I), single spill (S) and single plunger (P) for $\Delta f/f_0 = 0.73$.

use their data for these two points by making one assumption: that the atmospheric conditions were near neutral. We may then use Wu's[14] correlation of drag coefficients to estimate u_* from U_{10}. This we have done, and the results show that according to equation (3), $\Delta S/S$ between breaking events is in the range 0.04–0.09 for windspeeds in the range 6–12 m s^{-1} (Table 1). Thorpe and Humphries' data further imply that $\bar{x}$, their mean distance between breaking events, is comparable to the group length (see Fig. 3*d* of ref. 3).

Our laboratory measurements (Fig. 4) show that $\Delta S/S$ is approximately 0.1 for a single spilling break, where S here refers to the excess momentum flux carried by one group. The important feature of Fig. 4 is the rapid initial increase in $\Delta S/S$ with ak once the breaking threshold is passed. This implies that even the gentle breaking events contribute significant fractional losses in the momentum flux, comparable to those for a single spilling break.

We conclude that the excess momentum flux lost due to wave breaking may be comparable to that transferred from the wind. Further, our measurements imply that in future quantitive studies of wave breaking, it may be most fruitful to consider the dynamics of the breaking wave group rather than considering single breaking waves.

We thank Mr Eng-Soon Chan for collaboration on preliminary measurements and Dr Martin Greenhow for advice on the generation of breaking waves. This work is supported by NSF grants OCE-8214746 and MEA-8210169.

Received 28 May; accepted 25 July 1985.

1. Banner, M. L. & Melville, W. K. *J. Fluid Mech.* **77**, 825–842 (1976).
2. Thorpe, S. A. & Stubbs, A. R. *Nature* **279**, 403–405 (1979).
3. Thorpe, S. A. & Humphries, P. N. *Nature* **283**, 463–465 (1980).
4. Thorpe, S. A. *Phil. Trans. R. Soc.* A **304**, 155–210 (1982).
5. Longuet-Higgins, M. S. in *10th Symp. Naval Hydrodynamics*, 597–605, ONR, Arlington, Virginia (US Government Printing Office, 1976); in *Turbulent Fluxes through the Sea Surface, Wave Dynamics, and Prediction*, (eds Favre, A. & Hasselmann, K.) 199–220 (Plenum, New York, 1978).
6. Mitsuyasu, H. *J. geophys. Res.* **90**, 3343–3345 (1985).
7. Longuet-Higgins, M. S. & Cokelet, E. D. *Proc. R. Soc.* A**350**, 1–25 (1976).
8. Melville, W. K. *J. Fluid Mech.* **115**, 165–185 (1982).
9. Banner, M. L. & Phillips, O. M. *J. Fluid Mech.* **65**, 647–656 (1974).
10. Donelan, M., Longuet-Higgins, M. S. & Turner, J. S. *Nature* **239**, 449–451 (1972).
11. Melville, W. K., Rapp, R. J. & Chan, E. S. in *The Ocean Surface: Wave Breaking, Turbulent Mixing and Radio Probing* 413–418 (Reidel, Dordrecht, 1985).
12. Whitham, G. B. *Linear and Nonlinear Waves* (Wiley, New York, 1974).
13. Plant, W. J. *J. Geophys. Res.* **87**, 1661–1667 (1982).
14. Wu, J. *J. geophys. Res.* **87**, 9704–9706 (1982).

Magnetic differentiation of atmospheric dusts

F. Oldfield*, A. Hunt*, M. D. H. Jones*, R. Chester†, J. A. Dearing‡, L. Olsson§ & J. M. Prospero‖

Departments of *Geography and †Oceanography, University of Liverpool, PO Box 147, Liverpool L68 3BX, UK
‡ Department of Geography, Coventry Polytechnic, Coventry CV1 5FB, UK
§ Department of Physical Geography, University of Lund, Sölvegatan 13, S-22362 Lund, Sweden
‖ Department of Marine and Atmospheric Chemistry, University of Miami, 4600 Rickenbacker Causeway, Miami, Florida 33149, USA

Although several magnetic separation methods have been used to provide some initial subdivision and characterization of the particulate emission products of fossil-fuel combustion[1–5], only recently has there been any attempt to use magnetic properties to distinguish between different emission types[6,7] and atmospheric particulate sources[8]. In the present study, we use several concentration-independent magnetic parameters and ratios to characterize dusts from different source types. Non-destructive measurements of saturation isothermal remanence, anhysteretic remanence and frequency-dependent susceptibility differentiate atmospheric dusts into groups characterized by distinctive magnetic mineral and grain size assemblages. These assemblages can be related to the source of the dusts as they reflect differences in the conditions under which the magnetic oxides developed. The magnetic parameters are sensitive to differences between dusts arising from fossil-fuel combustion and from other industrial processes, and those derived from soil erosion. Within the set of soil-derived dusts, the magnetic parameters distinguish between the weathering regimes operating in different source areas.

Chester *et al.*[8] were able to distinguish between and characterize dust source types in the Mediterranean region by plotting aluminium concentration against the magnetic susceptibility/aluminium concentration quotient. Soil-derived dusts of North African origin fell at one extreme, with high aluminium concentrations and a low quotient, whereas urban/industrial dusts rich in magnetic spherules[9–11] fell at the opposite extreme. On a local scale, Hunt *et al.*[7], using magnetic parameters alone, were able to distinguish between fly ash originating from power stations and the particulates in automobile emissions. They were able to show consistent differences related to the coercivity of saturation isothermal remanence (see Fig. 1 legend). Such parameters, together with a range of interparametric ratios, have been used successfully to identify shifts in sediment source types in rivers[12,13], lakes[14] and a range of near-shore marine environments[15–17]; they are independent of concentration and can usually be measured rapidly and non-destructively on samples of 0.05 g or less.

Table 1 summarizes some of the measurements obtained for samples collected between October 1966 and July 1969 from the eastern tip of Barbados (13°10′ N, 59°30′ W) by means of 1 m × 0.5 m nylon mesh panels mounted on a 14-m-high platform and arranged so as to face the prevailing wind at all times[18,19]. Delaney *et al.*[18] regard the sampling efficiency of the method as being low for particles <1 μm in diameter. Out of a total of 20 samples received for magnetic measurement, four 'between-season' samples from October and November were omitted. The rest were identified as either red-brown, Sahara- and Sahel-derived 'summer' dusts, or grey, more locally derived, South American 'winter and spring' dusts[19,20]. The two populations are clearly distinguished on the basis of the parameters tabulated. For the Mann–Whitney U statistic, they show a significant difference at the $P = 0.05$ rejection level. The high coercivities of remanence (B_{CR}), 'harder' isothermal remanent magnetization (IRM)/saturation IRM (SIRM) quotients and higher SIRM/χ (low-field susceptibility) values for the Saharan set are consistent with a high haematite contribution typical of surface